

# Multi-Sensor Approach for Assessing the Taiga-Tundra Boundary

K.J. Ranson<sup>1</sup>, G. Sun<sup>2</sup>, V.I. Kharuk<sup>3</sup> and K.Kovacs<sup>4</sup>

<sup>1</sup> NASA's Goddard Space Flight Center, Code 923, Greenbelt, MD, USA, [kenneth.j.ranson@nasa.gov](mailto:kenneth.j.ranson@nasa.gov)

<sup>2</sup> Department of Geography University of Maryland, College Park, USA, [guoqing@taiga.gsfc.naa.gov](mailto:guoqing@taiga.gsfc.naa.gov).

<sup>3</sup> V.N. Sukachev Institute of Forest, Academgorodok, Krasnoyarsk, Russia, [kharuk@forest.akadem.ru](mailto:kharuk@forest.akadem.ru)

<sup>4</sup> Science Systems and Applications, Inc. Lanham, MD, USA, [kkovacs@forest.gsfc.nasa.gov](mailto:kkovacs@forest.gsfc.nasa.gov)

**Abstract-** Monitoring the dynamics of the tundra-taiga boundary is critical for our understanding of the causes and consequences of the changes in this area. Because of its inaccessibility, remote sensing data will play an important role. In this study we examined the use of several remote sensing techniques for identifying the existing tundra- taiga ecotone. These include Landsat, MISR and RADARSAT data. High-resolution IKONOS images were used for local ground truth.

It was found that on Landsat ETM+ summer images, reflectance from tundra and taiga at band 4 (NIR) is similar, but different at other bands such as red, and MIR bands. When the incidence angle is small, C-band HH-pol backscattering coefficients from both tundra and taiga are relatively high. The backscattering from tundra targets decreases faster than taiga targets when the incidence angle increases, because the tundra targets look smoother than taiga. Because of the shading effect of the vegetation, the MISR data, both multi-spectral data at nadir looking and multi-angle data at red and NIR bands, clearly show the transition zone.

*Keyword: Taiga-tundra transition zone, Landsat ETM+, RADARSAT, MISR*

## I. INTRODUCTION

The tundra-taiga boundary stretches for more than 13400 km around the Northern Hemisphere and is probably the Earth's greatest vegetation transition [1]. This transition zone (lesotundra zone) is sensitive to both climate change and human activities. Monitoring the dynamics of this tundra-taiga boundary is critical for our understanding of the causes and consequences of the changes.

There is great concern about the effect of human actions and climate changes on the landscape at the taiga-tundra transitional zone, but lack of effect method to map and monitor this zone. The mystery of a "missing sink" in global carbon balance emphasizes a need for new data, probably from satellite imagery, which offers much improved information on the area and changes in area and stature of forests [2]. Despite the lack of knowledge of the exact mechanism involved, there is general agreement that thermal characteristics of the climate

are of major importance in determining the northern edge of the boreal forest. Degradation of permafrost in many regions has been shown in numerous studies [3-4]. Recent observations by Siberian and other scientists suggest that the taiga forests are expanding into the tundra, an indicator of climate warming. Ground studies and remote sensing analysis are required to develop techniques to identify the establishment of taiga species in traditional tundra areas. In this study we examined the use of several remote sensing techniques for identifying the existing tundra-taiga ecotone.



Figure 1. View across the tundra taiga transition near Ary Mas, Russia

The Ary Mas (forest island) study site is located at 72° 1'N, 100° 50' E, in the tundra-taiga transition zone. This area is known as one of the most northerly places where larch can survive. Larch is the frontier species in this region. The local elevation and hydrology affect the tree distribution, including dendritic patterns along the river valleys. Figure 1. shows the general terrain across the tauundra-taiga ecotone. There is not an abrupt change between forest and tundra. Often trees colonize an area and slowly increase in crown cover.

Figure 2 presents the Landsat-7 ETM+ images of the site showing the ecotone between areas of light (tundra) and dark green taiga.

RADARSAT standard beam data at various incidence angles were acquire in August 2001 (see Table 1). Fig. 2. shows a false-color composite of RADARSAT data. Because of the higher

backscattering from trees at large incidence angles (ST5 and ST6), these areas are bright in the image. One IKONOS image within the area was also acquired and aided in interpretation.

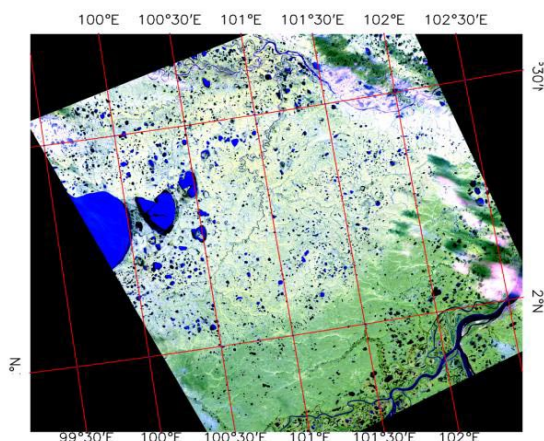


Figure 2. Landsat-7 ETM+ image (R-b7, G-b5, B-b3) of Ary-mas test site acquired on July 9, 1999. The image shows the transition from tundra to larch forest- colors from light green to dark green. There are clouds at upper-left corner and along right edge.

MISR data used in this study were acquired on August 23, 2001 and processed using HDF-EOS Data Format Converter (HEG) [5]. Figure 4 is a false composite of MISR Red band data. The forward-looking camera at  $70.5^\circ$  (DF) data is displayed as red, AN (nadir-looking) and DA ( $70.5^\circ$  backward-looking) as green and blue respectively. Because of the descending orbit and the southerly Solar azimuth the DF camera received specular (forward scattered) reflectance from water surfaces (red), and DA camera was near the hot-spot (backscatter) position. The tundra-taiga transition zone is also clearly shown in the MISR image.

TABLE I  
LIST OF REMOTE SENSING DATA USED IN THE STUDY.

Data	Acquisition Date	Characteristics
L-7 ETM+	07-09-1999	1-5,7 Bands
RADARSAT ST2	08-02-2001	$27.74^\circ$
ST3	08-05-2001	$34.10^\circ$
ST4	08-15-2001	$36.56^\circ$
ST5	08-08-2001	$39.22^\circ$
ET6	08-11-2001	$44.14^\circ$
IKONOS	07-17-2002	B,G,R,NIR, pan
MISR	08-23=2001	B,G,R,NIR 9 look angles

### III. DATA ANALYSIS AND RESULTS

All data were converted into Lambert Conformal Conical projection and registered together. Both ETM+ and MISR data were geo-referenced, and the RADARSAT data were manually registered to ETM+ data. In order to see how the signature changes across the boundary region, a profile of the data value was plotted for every channel. The profile is shown as the horizontal line in the center of Fig. 4. Total 400 pixels were extracted, which represent distance of 12 km in L-7 and RADARSAT images (30m pixel), and much longer in MISR image (100km). Some of these profiles were plotted in Fig. 5.

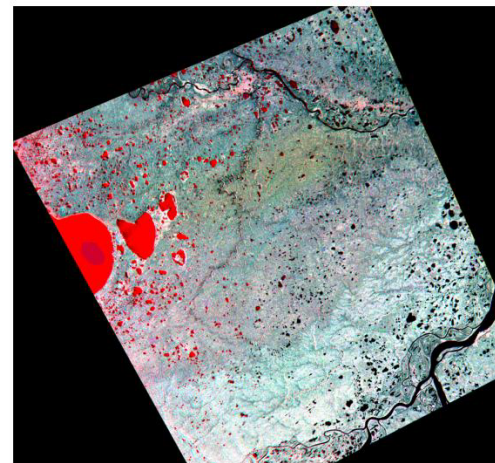


Figure 3. False-color RADARSAT data (R – ST2, G – ST6, B – ST5)

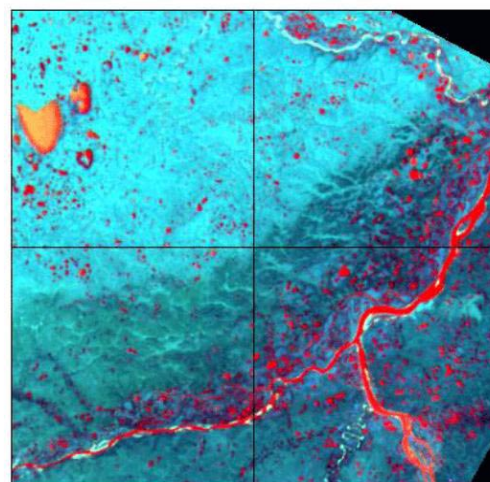


Fig. 4. MISR Red-band images (R – DF camera, G – AN, B – DA).

L-7 ETM+ bands 7,5, and 3 show the change across the tundra-taiga boundary. The other bands did not and are not plotted here. Across the transition zone from tundra to taiga, the reflectance at bands 7, 5, and 3 decreases. Radar backscattering is determined by plant water content, and the surface roughness. The lack of trees makes tundra appear smoother than taiga. At steeper incidence angle

(ST2), backscattering from both is relatively high. When incidence angle increases (ST5, 6), the backscattering from smoother surfaces, i.e. tundra, decreases faster. Both multi-spectral (nadir images) and multi-angle (in red band) MISR data show the transition zone. Red band responses from both forward (DF) and backward (DA) cameras show more significant change than the nadir looking image (lower-left plot in Fig. 5). Among the nadir looking MISR images, the red band shows the most significant change, which is consistent with L-7 ETM+ data.

To zoom in to the transition region and compare the changes in images of different sensors, the profiles of the most sensitive channels were registered in space and displayed in the same plot (Figure 6). For each channel the image value was normalized by the maximum value. The two L-7 curves were lowered by 0.2 and RADARSAT curves were lowered by 0.6 so these normalized curves could be separated in the plot. Along the 12-km profile, both ETM+ and RADARSAT data have 400 points, but MISR data only have about 48 points. The RADARSAT ST6 data shows most significant and consistent change in the boundary region. In addition to the vegetation change, other factors such as elevation and hydrological condition may also play a role here. The change patterns of ETM+ band 3 (red curve) and MISR red band DA image (dark purple curve) are very similar. The vertical line identifies the center of the profile (see Figure 4).

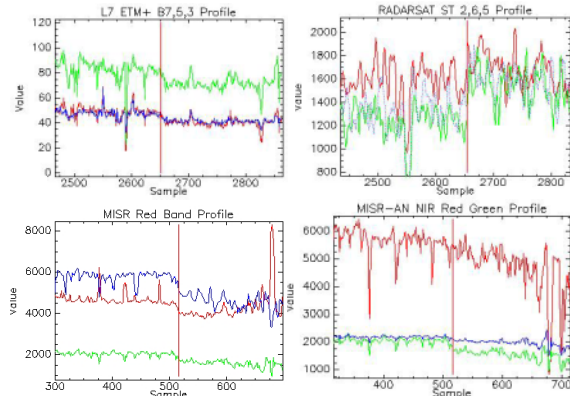


Figure 5. Signature profiles for ETM+, RADARSAT CHH and MISR. The vertical line is the center of the profile. Upper-left is ETM+ data with bands 7,5,3 as RGB. Upper-right is CHH data with ST2,6,5 as RGB. Lower-left is MISR red bands with cameras DF, AN, DA as RGB, and lower-right is MISR nadir image (AN) with bands NIR, red and green as RGB.

#### IV. CONCLUDING REMARKS

This study has shown that data from L-7 ETM+ red and mid-infrared bands, MISR red band forward and backward looking cameras, and RADARSAT larger incidence angle images are sensitive to the

surface and vegetation structure change in tundra-taiga transition zone. The location of the transition zone identified as a change in spectral response from images with very different spatial resolutions was consistent. Our further studies will focus on the mapping and characterization of this transition zone from these remotely sensed data. Since topography has an important role in controlling the location of these transition areas we will incorporate this into later analyses.

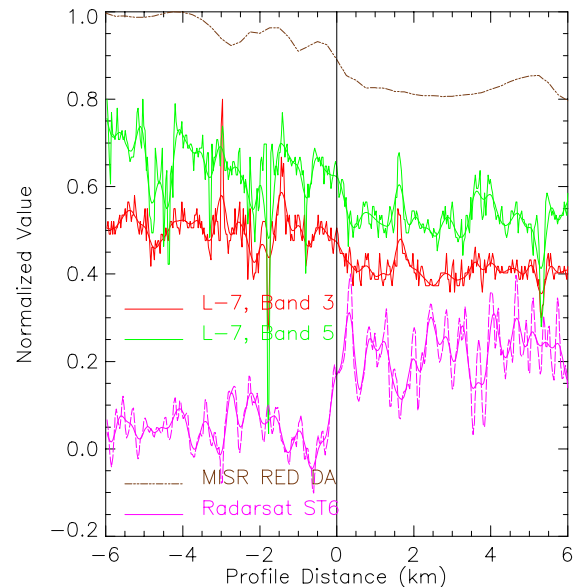


Figure 6. Signature profiles of ETM+, RADARSAT and MISR data across a tundra-taiga transition boundary.

#### V. REFERENCES

- [1] T. V. Callaghan, R. M. M. Crawford, M. Eronen, A. Hofgaard, S. Payette, W. G. Rees, O. Skre, B. Sveinbjornsson, T. K. Vlassova and B. R. Werkman, The dynamics of the tundra-taiga boundary: An overview and Suggested coordinated and integrated approach to research, AMBIO, Special Report 12, tundra-Taiga Treeline Research, pp. 3-5, 2002.
- [2] G. Rees, I. Brown, K. Mikkola, T. Virtanen, and B. Werkman, How can the dynamics of the tundra-taiga boundary Be remotely monitored? AMBIO, Special Report 12, tundra-Taiga Treeline Research, pp. 56-62, 2002.
- [3] T. E. Osterkamp, and V.E. Romanovsky. Impacts of thawing permafrost as a result of climatic warming, EOS, Trans. AGU. 77(46), F188, 1996.
- [4] A. V. Pavlov, Current changes of climate and permafrost in the Arctic and Sub-Arctic of Russia. Permafrost and Periglacial Processes. 5:101-110, 1994.
- [5] Raytheon Systems Company, HDF-EOS Data Format Converter (HEG) Users Guide, v 1.0, Technical Paper 170-TP-013-001, January, 2003.